Journal of Ultrafine Grained and Nanostructured Materials
https://jufgnsm.ut.ac.ir
Vol. 54, No.1, June 2021, pp. 93-100
Print ISSN: 2423-6845 Online ISSN: 2423-6837
DOI: 10.22059/jufgnsm.2021.01.10

In vitro Corrosion Behavior and Biological Properties of Magnesium-Zinc-Calcium Alloy Coated with Polycaprolactone Nanofibers

SeyedeHosna Hadavi[1], Reza Soltani*[*,1], Elnaz Tamjid[2], Rouhollah Mehdinavaz Aghdam[1]

[1]School of Metallurgy and Materials Engineering, College of Engineering, University of Tehran, Tehran, Iran.
[2]Department of Nanobiotechnology, Faculty of Biological Sciences, Tarbiat Modares University, Tehran, Iran.

Recieved: 27 January 2021; Accepted: 11 May 2021
** Corresponding author email: rsoltani@ut.ac.ir*

ABSTRACT

Magnesium alloys have received great attention for the medical applications such as bone implants mainly due to high biocompatibility and mechanical properties. But the main challenge of using magnesium alloys is its high rate of degradation. Many researches have been focused on how to control the corrosion rate of these alloys and in this work, the nanofibers of polycarprolactone were applied by electrospining technique onto the Mg-4Zn-2Ca alloy as a thin coating to reduce corrosion rate. The Tafel polarization test showed that the applied coating reduced the corrosion rate by about two order of magnitudes. The amount of hydrogen released by the corrosion reactions in the coated sample was much less than that of the uncoated sample. Biocompatibility test showed that 8% less cytotoxicity of the coated sample compared to the uncoated ones. In the cell adhesion test, it was observed that much more cells adhere onto the coating rather than uncoated sample. coating Mg alloys with this material and morphology could have some advantages for future implants.

Keywords: *Magnesium alloy; Polycaprolactone polymer; Electrospinning; In vitro corrosion; Biocompatibility.*

1. Introduction

The history of the using the metal implants dates back to the nineteenth century as the Industrial revolution led to the expansion of the use of metals in life. Since then, biological metallic materials have always been designed to be corrosion resistant [1,2]. For decades, this pattern has become a major part of the biomaterial's world. Recently, with the advancement of tissue engineering, biological materials were predicted to actively interact with the body [3]. Metallic biomaterials no longer need to be ineffective, but they should be able to help and enhance the healing process. In many cases, the biomaterial must do its job and then leave the area. This idea opened a new horizon and offered a new insight. It is conceivable to design a material that can provide mechanical support for the required period of time and then gradually degrade. This idea directly breaks the pattern of corrosion-resistant biomaterials [4,5].

Some specific clinical problems require only temporary support provided by implants made of biodegradable materials that allow the implant to be degraded gradually after its function [6] such as degradable sutures [7,8]. However, degradable implants, especially those made of metal, could be considered a new concept and refute the old hypothesis that a metal biomaterial must be corrosion resistant [9].

Magnesium and its alloys are biological metallic

materials that can be degraded in body fluids and are also an essential element for bone metabolism and may cause formation of new bone tissue. In addition, the elastic modulus of magnesium alloys is more compatible with natural bone than other metals, as a result, it reduces the stress on the normal bone [10]. Also, magnesium ion is the fourth most abundant cation in the human body and to a large extent in tissues Bone is stored [11].

The rapid degradation of magnesium alloys, increases the likelihood of losing mechanical stability before bone tissue healing [12]. This also may cause hydrogen gas accumulation around magnesium implants, loosening the implants. Recently, some studies have focused on reducing the rate of degradation of magnesium alloys and its biocompatibility [13].

Biocompatible polymers are also very desirable to be used as implants. But since they have low strength, they should be placed on the surface of metals [14]. These polymers can be extruded as Nanofibers and then placed on the metallic surfaces. Fibers are generally classified into three categories: ordinary fibers, micro fibers, and nanofibers. When the diameter of polymer fibers was reduced from a micron to a few hundred nanometers, amazing properties such as very high surface-to-volume ratio, high porosity, good flexibility, high permeability, very low weight and high mechanical efficiency will be obtained in materials [15,16]. Such prominent features make nanofibers a suitable choice for many important applications [17]. new generation of magnesium alloys containing zinc and calcium elements with positive roles, have received great attentions recently. In this job magnesium-zinc-calcium alloy [18,19] was used as the substrate and electrospinning method was selected to produce and coat polycaprolactone nanofibers on the substrates [20,21].

The coating corrosion behavior was studied by Tafel polarization and hydrogen release tests along with cytotoxicity, cell adhesion, and pH change tests.

2. Materials and Methods

2.1. Material selection and preparation process

The ingot of magnesium-zinc-calcium alloy was cast with the chemical composition of 2.4 to 5.4 wt.% zinc and 1.2 to 8.1 wt.% calcium in a controlled atmosphere condition. The square samples were wire cut from the ingot to the size of 0.5 × 1 × 1 cm samples. Then the samples were grinded with 180 grit SiC sandpaper prior to any test and coating process.

First, the solvent was prepared by combining chloroform (1.48 gr/cm^3) with methanol (0.792 gr/cm^3) in a ratio of 3 to 1. Then 10 vol.% of The PCL (Poly Capro Lactone) granules were added to the solvent. The mixture was stirred with a magnetic stirrer for 2 hours to obtain a homogenous mixture prepared for producing nanofibers by electrospinning. The samples were glued to the drum of the electrospinning device (model ES1000, Iran) in a way that the electrical connection between the drum and the specimens was maintained [22,23]. FESEM analysis was used to evaluate the fibers obtained from the electrospinning. The diameter of each fiber was measured using ImageJ graphic software.

2.2. Corrosion tests

Tafel polarization (by GU140NR model) and hydrogen tests were performed (three times) in the simulated body fluid (SBF) [24] at a temperature of 37 ° C, to compare the corrosion behavior of uncoated and coated samples. For the electrochemical corrosion cell, platinum was used as the counter electrode, the saturated calomel electrode (SCE-Ag / AgCl) as the reference electrode and the sample as the working electrode. Polarization curves with potential scanning were obtained from -250 to +250mV at a scanning rate of 1 mV/s at 37 °C [25]. For better understanding the difference in the corrosion behavior, the change in sample thickness due to the corrosion during one year can be calculated by placing the corrosion intensity from the polarization test in Equation 1 [26].

$$r_{corr.} = 0.0032 \times A \times Mw / n \times d \quad (1)$$

where A is the current intensity in microamperes per square centimeter (mA.cm^{-2}), Mw is the molar mass of matter, n is the number of electrons exchanged, and d is the density of matter, so the unit of corrosion rate is equal to millimeters per year.

As stated before, magnesium is ionized in the presence of the SBF based on an electrochemical anodic reaction and then is converted to magnesium hydroxide by reacting with a hydroxyl ion; as a result, hydrogen gas evolution occurs according to Equation 2 [27,28].

$$Mg + 2H_2O \rightarrow Mg(OH)_2 + H_2 \quad (2)$$

Therefore, measuring the emitted hydrogen gas can be a measure of the degree of corrosion of the part. In this test, each of the two groups of coated and uncoated samples were placed inside a beaker and a funnel was placed on the samples for the suction of the emitted gas. Beaker was placed in a SHIMAZ water bath at room temperature. Beaker and burettes were filled with 400 and 100 ml of the SBF, respectively. The laboratory burette was placed upside down on each funnel to collect released hydrogen gas. The height of the solution inside the port was measured at different times for 9 consecutive days. Whenever the height of the solution reached zero, it was refilled with the solution inside the beaker. For the accuracy of the final results, the total volume of solution inside the beaker and the burette was kept 500 ml in this study.

With the help of the difference in the height of the solution in the port at different time intervals, equations 3 and 4 can be used to calculate the corrosion rate of each sample [29].

$$r_{corr.} = 2.088 \times 24 \times (\Delta H \text{ total} \times A) / \Delta t \quad (3)$$

$$\Delta H \text{ total} = (h_1 - h_2) + H_1 \quad (4)$$

where A is the cross-sectional area of the sample (cm^2), ΔH total the reaction height, Δt the elapsed time (hour), and h the height of the solution inside the port.

Intense corrosion upon exposure to the body fluid, results in hydroxyl ion (OH^-) release. Hydroxyl ions cause the environment of the body to become alkaline which affects the survival of the cells in the body towards possibility increase of cell death. Therefore, the pH of the SBF was recorded daily by a PH meter (model PH-98107) to plot its changes over time for each sample. 3 times repeating experiments under same conditions, made the results more reliable.

2.3. Cytotoxicity test

NCBI C555 (MG-63) cells were used in this analysis. After defrosting the cells and transferring them to a flask containing DMEM 2 medium with 10% SBF, the flask was kept at 37 °C for incubating. Humidity of 90% and concentration of carbon dioxide 5% were set and the culture medium was changed every 3-4 days.

In order to investigate the toxicity of the samples and their effect on cell growth and proliferation, the extraction process was performed according to ISO 599993 standard, during which the samples were first sterilized by UV irradiation. To the surface of each sample, 1 ml of culture medium per cm^2 of the surface was added. Then, after 3 days, the medium was removed and added to the cells. A certain amount of DMEM culture medium was also considered as a control sample.

One of the best indirect method available for determining cell proliferation is the dimethyl thiazole diphenyltetrazolium bromide (MTT, Sigma, USA) test, which is based on the change of tetrazolium yellow powder to insoluble purple-black crystals of Formazan. Formazan crystals are soluble in organic solvents such as isopropanol, and the resulting optical density (OD) is read using an ELISAR device. The optical density is directly proportional to the concentration of formazan, which is proportional to the metabolic activity of living cells. In this study, to evaluate the rate of cell proliferation, first 1×10^4 cells with 100 µl of culture medium were poured into each well of a 96-well cell culture plate and then incubated at 37 °C for 24 hours to allow the cells to adhere to the bottom of the plate.

After ensuring the adhesion of the cells, the culture medium was removed from the cells as much as possible and 90 µl of the prepared extracts as well as the extracts diluted with the culture medium along with 10 µl of SBF were added to each culture well and the cells for 24 hours. The culture medium was then removed and 100 µl of MTT at a concentration of 0.5 mg / ml was poured into each well and incubated for 4 h. then solution was removed from the cells and isopropanol was added to dissolve the purple crystals. To better dissolve the MTT precipitate, the plate was placed on a shaker for 15 minutes. Then the concentration of the solute in isopropanol was calculated using an ELISA device (STAT FAX 2100, USA) at 545 nm.

The well with more cells shows higher optical density (OD) than the well with less cells. Eq. 5 and 6 help to determine the toxicity and viability. It should be noted that each sample had 6 replications.

$$\text{Toxicity\%} = (1 - \text{mean OD of sample}) \times 100 \text{ mean OD of control} \quad (5)$$

$$\text{Viability\%} = 100 - \text{Toxicity\%} \quad (6)$$

2.4. Cell adhesion test

To check cell adhesion, sterilized samples were first placed in each of the 24-well plate sterile wells. Then 30,000 cells in a volume of 50 microliters were poured on each sample and incubated for 4-5 hours. After the cells adhered, a certain amount of culture medium including 10% SBF was added to each well. After 24 hours, the culture medium was removed from the samples and washed with PBS (Phosphate-buffered saline) for 30 seconds. Then 5.3% glutaraldehyde was used for cell fixation. After pouring a certain amount of fixative on each sample, they were placed in the refrigerator for 2 hours and then the fixative was removed and the samples were divided into 2 series which were washed with deionized water and alcohols of 50%, 60%, 70%, 80% and 96%. The cell adhesion to the samples was then examined by 15 Evo Ma (Zeiss) scanning electron microscopy.

3. Results and Discussion

3.1. Morphology of electrified fibers

As shown in Fig. 1 the final fiber diameter was about 74± 15 nm, so it can be said that the resulting fibers are nano scale in diameter. The nano porosity in the coating (among fibers) provides a good place for tissue growth and also delaying SBF to reach the metal and start corrosion process. This also provides more time for curing damaged organs.

3.2. Tafel polarization test

The Evan diagram from Tafel polarization test (Fig. 2) shows the relationship of current and potential for oxidation and reduction reactions; so it is the best choice for comparison corrosion behavior between different cases. As shown in the figure, the corrosion current density of the coated sample is less than that of the uncoated sample and its corrosion potential (-0.66 volts vs SCE) is more positive than that of the uncoated sample (-1.52 volts vs SCE), which both of them indicate better corrosion resistance of the coated sample compared to the uncoated one.

An increase of about 0.9 V means that corrosion of the coated sample occurs at higher potentials and the sample is stable in the higher potential range and does not enter the corrosion zone. Also, the corrosion current density, which indicates the corrosion rate for the uncoated sample is 2.8×10^{-4} $A.cm^{-2}$ whereas this density for the coated sample is 1.5×10^{-6} $A.cm^{-2}$, indicating a corrosion resistance of almost two order of magnitude higher than the bare alloy.

The corrosion mechanism of the magnesium alloy sample in this study consisted of at least two electrochemical reactions as anodic and cathodic according to Equations 7 to 9. The used alloy, contains about 94 wt% magnesium, 4 wt% zinc and 2 wt% calcium. All three elements are anodic in the standard state relative to hydrogen, and therefore zinc and calcium can be expected to convert to zinc and calcium ions in the anodic reaction and release electrons. The electron reacts with the hydrogen ion at the cathode surface and hydrogen gas is released.

$$Mg \rightarrow Mg^{2+} + 2e^{-} \quad (7)$$

$$2H^{+} + 2e^{-} \rightarrow H_2 \quad (8)$$

$$H_2 + Mg^{2+} \rightarrow H_2^{+} + Mg \quad (9)$$

Based on the test conditions (ambient temperature and pressure) and assuming concentration of magnesium ions equal to 1 (since the used alloy contains about 94% by weight of magnesium) the

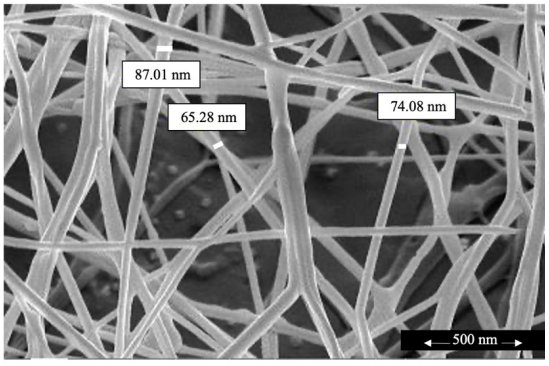

Fig. 1- FESEM image of Nanofibers of polycaprolactone obtained from electrospinning process.

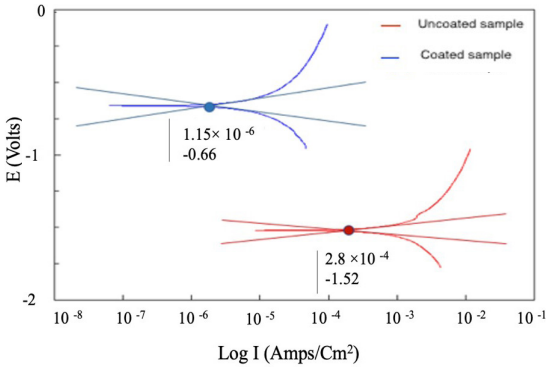

Fig. 2- Evan's diagram from Tafel polarization tests of the coated and uncoated samples.

concentration of hydrogen ions is calculated from the pH of the test solution, which is 7.2. The Nernst equation, Equation 10, can be used to calculate the potential in such a situation where E_o is the standard potential.

$$E = E_0 - \left(\frac{0.059}{2}\log\frac{[Mg^{2+}]}{[H^+]^2}\right) \quad (10)$$

$$E = E_0 - 0.059\,pH \quad (11)$$

The standard electrode potential of magnesium in the reduction reaction of magnesium ion is -37.2 volts [31], and consequently in the reaction of equation 11 is equal to + 37.2 and at pH = 7.2 the reaction potential is equal to + 9.1 volts. So, because:

$$\Delta G = -nFE \quad (12)$$

Where n is the number of electron moles and F is the Faraday constant, with positive potential, negative free energy is obtained; In other words, the reaction 12 is possible. On the other hand, OH^- ions are present in the environment and the release of magnesium ions causes a reaction based on the equations 13 and 14:

$$Mg^{2+} + OH^- \rightarrow Mg(OH)_2 \quad (13)$$

$$Mg(OH)_2 + 2Cl^- \rightarrow Mg(Cl)_2 + OH^- \quad (14)$$

Although magnesium hydroxide can provide some degree of surface protection on the surface of magnesium, but its conversion to magnesium chloride removes this protection. As a result, corrosion of magnesium is intensified in the presence of chlorine ions [27].

Any factor that delays the formation of magnesium ions reduces the corrosion of the base metal and its alloy. The continuous layer of polycaprolactone polymer prevents the corrosive electrolyte from reaching the surface of magnesium alloy, therefore reducing magnesium ions production and consequently increasing its corrosion resistance. The results obtained in the polarization test also confirms this conclusion.

Coating as a homogeneous layer by covering the sample surface, prevents the solution from reaching and ion exchange in the coated sample. Inhibition of ion transfer creates a type of concentration polarization in the solution and in the vicinity of the coating layer, requiring higher potentials to re-form the corrosion circuit; Therefore, by this way the substrate is protected [31].

3.3. The hydrogen gas evolution measurement

Based on the equations (3) and (4), the amount of corrosion per year (mpy) was calculated and plotted against exposure time (Fig. 3).

As it is seen, the corrosion rate of the uncoated sample is much higher than the coated one. On the fifth day, the corrosion rate of the uncoated and coated samples is 300 and 50 mpy, respectively. This means that the polymer coating was able to create a large barrier between the electrolyte and the magnesium alloy surface.

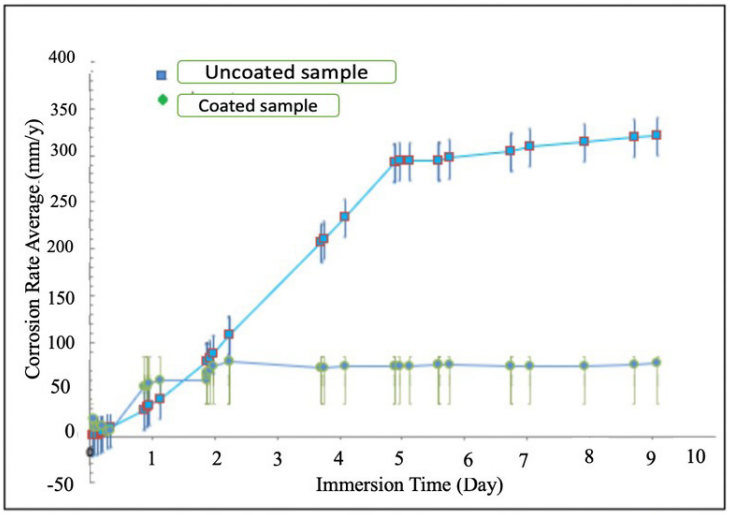

Fig. 3- Changing the corrosion rate with the retention time in the solution by monitoring the amount of hydrogen released during the corrosion test.

For the first five days the corrosion rate increases rapidly and then drops to lower levels. A sharp increase in corrosion rate could be due to-the lack of protection of the sample against corrosive media. However, over time, the decrease in the slope of the corrosion rate can be related to the gradual formation of corrosion products, which can, to some extent, play the role of protecting the sample against corrosion. The reduction of corrosion rate after 5 days could also be due to the concentration polarization, where hydrogen bubbles could not leave the cathode surface, and hence, retard the cathodic reactions. In turn, the anodic reaction reduces as the total anodic and cathodic reaction rates should be the same.

3.4. pH changes of the SBF

The pH changes of the body simulated fluid adjacent to the coated and uncoated samples were measured over time in 7 consecutive days and the results are shown in Figure 4. Cells need a pH of about 7 to grow, and due to the reactions, that occur between the sample and the surrounding environment, hydroxide ions and chlorine ions are released, which increase the pH of the environment and this endangers the survival of the cells.

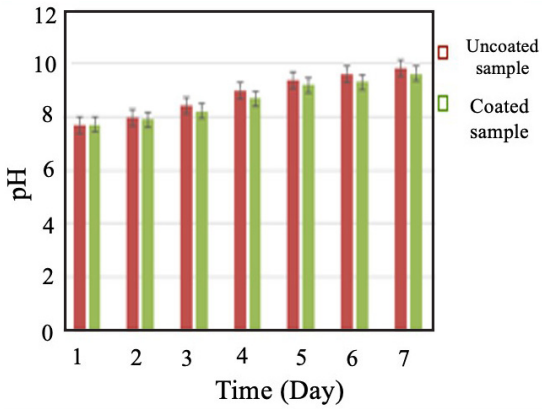

Fig. 4- Change of pH of SBF over time due to the reaction of the coated and uncoated samples with SBF.

As a result, the smaller the pH changes, the better for cell growth. As shown in the figure 4, changes in the pH of the SBF over time in the coated sample are less than that in the uncoated one due to the delay in the formation of magnesium hydroxide by the polycaprolactone coating, resulting in a decrease in the amount of chlorine ions released [32].

3.5. Biocompatibility test results

Cytotoxicity test was performed by direct cell contact (MG-63) NCBI C555 on uncoated and coated magnesium alloy samples by MTT (3-(4,5-di- methylthiazol-2-yl)-2,5-diphenyl tetrazolium bromide) method. As shown in Figure 5, at the main concentration, the cytotoxicity of the coated sample is 8% less than that of the uncoated sample, but by diluting the two samples, the cell viability in both samples is calculated to be approximately the same. The obtained data show that the nanofiber network provides a suitable environment for cell growth and proliferation, in agreement with the literature [34].

Therefore, another factor that reduces the number of cells and, consequently, the percentage of adsorption in the uncoated sample, can be severe changes in pH.

3.6. Cell adhesion

Using the method mentioned previously, the MG-63 (NCBI C555) cell was placed on the surface of both coated and uncoated samples, and their characteristics were studied using a scanning

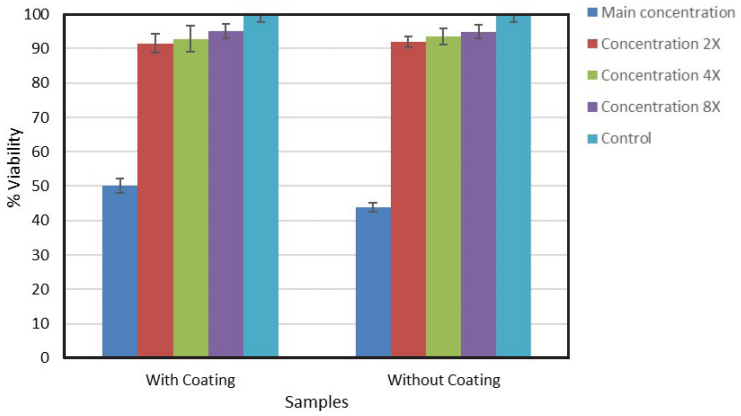

Fig. 5- Comparison of cell viability with MTT test on samples.

electron microscope. As Fig. 6 shows, the cell coverage, density, and adhesion in the coated surface were more than those in the uncoated sample. The greater the extent of the cells on the surface shows the more suitability of the surface for cell growth. Surface energy plays an important role in cellular interactions. A substrate with a higher energy level and optimal roughness absorbs protein, which helps the cell to proliferate and adhere better [35,36].

The presence of porosity in the surface layer can be effective in leading cells to proliferation and differentiation. Table 1 shows a comparison between the cells at the level of the two samples.

The cells adhering to the surface of the specimens are less than 15 micrometers, and as can be seen, the coated specimen has far more cells adhered to the surface than the uncoated specimen due to the presence of polycaprolactone polymer, which has a high biocompatibility property. The placement of this coating in the form of nanofibers causes more cell adhesion to the surface [37,38].

4. Conclusions

In this work, the aim was to improve the in vitro corrosion behavior of Mg alloy by coating polycaprolactone polymer nanofibers on its surface. The coating was applied by choosing appropriate parameters on the electrospinning device.

By controlling the electrospinning conditions, the diameter of the fibers was measured approximately less than 100 nm and therefore they can be classified as nanofibers. The results of Tafel polarization test showed that the process increased the corrosion potential from -1.5 to -0.6 V (vs SCE), whereas the corrosion current density was lowered about at least one order of magnitude. The hydrogen test showed that after a few days of immersing the samples in the simulated body fluid, the corrosion products play the role of surface protection and the corrosion rate decreased. It also showed that the amount of hydrogen emitted from the corrosion reaction of the samples in the coated sample is much less than the uncoated sample. In the pH test of the body simulation solution, when the samples were exposed to this solution for 7 days, it was observed that the solution in which the coated sample was located had a lower pH increase, although the difference between the pH increase in the two solutions was not very large, but this is very important in the survival of cells. The results of biocompatibility test showed that at the main concentration, the cytotoxicity of the coated sample was 8% less than the uncoated sample,

Table 1- comparison of the number of cells attached to 1 cm^2 of the surface of samples

Sample	Coated sample	Uncoated sample
Number of cells attached to the surface	150 ± 15	50 ± 10

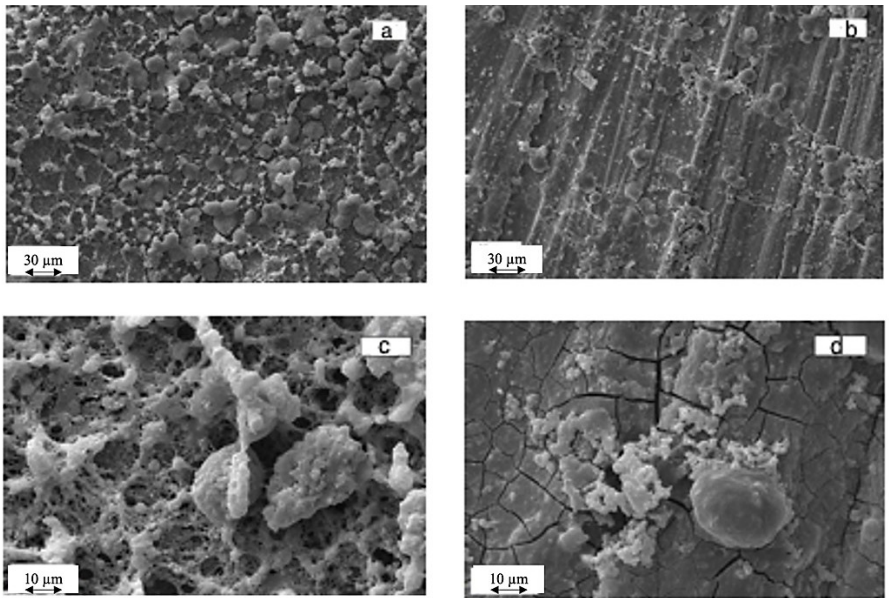

Fig. 6- SEM images with two different magnifications to check cell adhesion to (a) and (c) coated specimens, (b) and (d) uncoated specimens.

but by diluting the two samples, the cell viability in both samples was found to be almost the same. Based on the results obtained from the SEM images of the cell adhesion test, it was found that the coated specimen possessed far more adherent cells than the uncoated specimen, which proved that the cell adhesion of the coated specimen was higher than that of the uncoated specimen.

References

1. Biomaterials. CRC Press; 2012.
2. Witte F. The history of biodegradable magnesium implants: A review. Acta Biomaterialia. 2010;6(5):1680-92.
3. Niinomi M. Recent metallic materials for biomedical applications. Metallurgical and Materials Transactions A. 2002;33(3):477-86.
4. Williams DF, editor. Progress in Biomedical Engineering: Definitions in Biomaterials. Elsevier; 1987.
5. Hermawan H. Biodegradable Metals for Cardiovascular Applications. Biodegradable Metals: Springer Berlin Heidelberg; 2012. p. 23-37.
6. Saris N-EL, Mervaala E, Karppanen H, Khawaja JA, Lewenstam A. Magnesium. Clinica Chimica Acta. 2000;294(1-2):1-26.
7. Okuma T. Magnesium and bone strength. Nutrition. 2001;17(7-8):679-80.
8. Vormann J. Magnesium: nutrition and metabolism. Molecular Aspects of Medicine. 2003;24(1-3):27-37.
9. Park J, Lakes RS. Biomaterials: an introduction. Springer Science & Business Media; 2007 Jul 23.
10. Apple DJ, Mamalis N, Brady SE, Loftfield K, Kavka-Van Norman D, Olson RJ. Biocompatibility of implant materials: A review and scanning electron microscopic study. American Intra-Ocular Implant Society Journal. 1984;10(1):53-66.
11. Staiger MP, Pietak AM, Huadmai J, Dias G. Magnesium and its alloys as orthopedic biomaterials: A review. Biomaterials. 2006;27(9):1728-34.
12. Jacobs JJ, Gilbert JL, Urban RM. Corrosion of Metal Orthopaedic Implants*. The Journal of Bone and Joint Surgery (American Volume). 1998;80(2):268-82.
13. Chen Q, Thouas GA. Metallic implant biomaterials. Materials Science and Engineering: R: Reports. 2015;87:1-57.
14. Kasemo B. Biocompatibility of titanium implants: Surface science aspects. The Journal of Prosthetic Dentistry. 1983;49(6):832-7.
15. Nguyen LTH, Chen S, Elumalai NK, Prabhakaran MP, Zong Y, Vijila C, et al. Biological, Chemical, and Electronic Applications of Nanofibers. Macromolecular Materials and Engineering. 2012;298(8):822-67.
16. Tamai H, Igaki K, Kyo E, Kosuga K, Kawashima A, Matsui S, et al. Initial and 6-Month Results of Biodegradable Poly- l -Lactic Acid Coronary Stents in Humans. Circulation. 2000;102(4):399-404.
17. Magnesium Technology 2013. John Wiley & Sons, Inc.; 2013.
18. Zhang L-N, Hou Z-T, Ye X, Xu Z-B, Bai X-L, Shang P. The effect of selected alloying element additions on properties of Mg-based alloy as bioimplants: A literature review. Frontiers of Materials Science. 2013;7(3):227-36.
19. Ding Y, Wen C, Hodgson P, Li Y. Effects of alloying elements on the corrosion behavior and biocompatibility of biodegradable magnesium alloys: a review. J Mater Chem B. 2014;2(14):1912-33.
20. van der Giessen WJ, Lincoff AM, Schwartz RS, van Beusekom HMM, Serruys PW, Holmes DR, et al. Marked Inflammatory Sequelae to Implantation of Biodegradable and Nonbiodegradable Polymers in Porcine Coronary Arteries. Circulation. 1996;94(7):1690-7.
21. Qin X, Wu D. Effect of different solvents on poly(caprolactone) (PCL) electrospun nonwoven membranes. Journal of Thermal Analysis and Calorimetry. 2011;107(3):1007-13.
22. Tan SH, Inai R, Kotaki M, Ramakrishna S. Systematic parameter study for ultra-fine fiber fabrication via electrospinning process. Polymer. 2005;46(16):6128-34.
23. Panahi Z, Tamjid E, Rezaei M. Surface modification of biodegradable AZ91 magnesium alloy by electrospun polymer nanocomposite: Evaluation of in vitro degradation and cytocompatibility. Surface and Coatings Technology. 2020;386:125461.
24. Kokubo T, Takadama H. How useful is SBF in predicting in vivo bone bioactivity? Biomaterials. 2006;27(15):2907-15.
25. Reifenrath J, Bormann D, Meyer-Lindenberg A. Magnesium Alloys as Promising Degradable Implant Materials in Orthopaedic Research. Magnesium Alloys - Corrosion and Surface Treatments: InTech; 2011.
26. Fukumoto S, Sugahara K, Yamamoto A, Tsubakino H. Improvement of Corrosion Resistance and Adhesion of Coating Layer for Magnesium Alloy Coated with High Purity Magnesium. MATERIALS TRANSACTIONS. 2003;44(4):518-23.
27. Witte F, Hort N, Vogt C, Cohen S, Kainer KU, Willumeit R, et al. Degradable biomaterials based on magnesium corrosion. Current Opinion in Solid State and Materials Science. 2008;12(5-6):63-72.
28. Maguire ME, Cowan JA. BioMetals. 2002;15(3):203-10.
29. Bahmani A, Arthanari S, Shin KS. Formulation of corrosion rate of magnesium alloys using microstructural parameters. Journal of Magnesium and Alloys. 2020;8(1):134-49.
30. Ho Y-H, Vora HD, Dahotre NB. Laser surface modification of AZ31B Mg alloy for bio-wettability. Journal of Biomaterials Applications. 2014;29(7):915-28.
31. Corrosion by Liquid Metals. Corrosion: Fundamentals, Testing, and Protection: ASM International; 2003. p. 129-34.
32. Perrault GG. The potential-pH diagram of the magnesium-water system. Journal of Electroanalytical Chemistry and Interfacial Electrochemistry. 1974;51(1):107-19.
33. Sunil BR, Kumar AA, Sampath Kumar TS, Chakkingal U. Role of biomineralization on the degradation of fine grained AZ31 magnesium alloy processed by groove pressing. Materials Science and Engineering: C. 2013;33(3):1607-15.
34. Razavi M, Fathi M, Savabi O, Vashaee D, Tayebi L. In vivo biocompatibility of Mg implants surface modified by nanostructured merwinite/PEO. Journal of Materials Science: Materials in Medicine. 2015;26(5).
35. Soujanya GK, Hanas T, Chakrapani VY, Sunil BR, Kumar TSS. Electrospun Nanofibrous Polymer Coated Magnesium Alloy for Biodegradable Implant Applications. Procedia Materials Science. 2014;5:817-23.
36. Cui W, Zhou Y, Chang J. Electrospun nanofibrous materials for tissue engineering and drug delivery. Sci Technol Adv Mater. 2010;11(1):014108-.
37. Zreiqat H, Howlett CR, Zannettino A, Evans P, Schulze-Tanzil G, Knabe C, et al. Mechanisms of magnesium-stimulated adhesion of osteoblastic cells to commonly used orthopaedic implants. Journal of Biomedical Materials Research. 2002;62(2):175-84.
38. Yamasaki Y, Yoshida Y, Okazaki M, Shimazu A, Uchida T, Kubo T, et al. Synthesis of functionally graded MgCO3 apatite accelerating osteoblast adhesion. Journal of Biomedical Materials Research. 2002;62(1):99-105.